Scientific Research Publishing

Advances in Chemical Engineering and Science, 2023, 13, 250-264
https://www.scirp.org/journal/aces
ISSN Online: 2160-0406
ISSN Print: 2160-0392

An Experimental Observation of the Thermal Effects and NO Emissions during Dissociation and Oxidation of Ammonia in the Presence of a Bundle of Thermocouples in a Vertical Flow Reactor

Samuel Ronald Holden[1*], Zhezi Zhang[1], Jian Gao[2], Junzhi Wu[1,3], Dongke Zhang[1]

[1]Centre for Energy (M473), The University of Western Australia, Perth, Australia
[2]College of Urban Transportation and Logistics, Shenzhen Technology University, Shenzhen, China
[3]Shanxi Institute of Energy, Taiyuan, China
Email: *sam.holden@research.uwa.edu.au

How to cite this paper: Holden, S.R., Zhang, Z.Z., Gao, J., Wu, J.Z. and Zhang, D.K. (2023) An Experimental Observation of the Thermal Effects and NO Emissions during Dissociation and Oxidation of Ammonia in the Presence of a Bundle of Thermocouples in a Vertical Flow Reactor. *Advances in Chemical Engineering and Science*, **13**, 250-264.
https://doi.org/10.4236/aces.2023.133018

Received: May 8, 2023
Accepted: July 28, 2023
Published: July 31, 2023

Abstract

Ammonia (NH_3) dissociation and oxidation in a cylindrical quartz reactor has been experimentally studied for various inlet NH_3 concentrations (5%, 10%, and 15%) and reactor temperatures between 700 K and 1000 K. The thermal effects during both NH_3 dissociation (endothermic) and oxidation (exothermic) were observed using a bundle of thermocouples positioned along the central axis of the quartz reactor, while the corresponding NH_3 conversions and nitrogen oxides emissions were determined by analysing the gas composition of the reactor exit stream. A stronger endothermic effect, as indicated by a greater temperature drop during NH_3 dissociation, was observed as the NH_3 feed concentration and reactor temperature increased. During NH_3 oxidation, a predominantly greater exothermic effect with increasing NH_3 feed concentration and reactor temperature was also evident; however, it was apparent that NH_3 dissociation occurred near the reactor inlet, preceding the downstream NH_3 and H_2 oxidation. For both NH_3 dissociation and oxidation, NH_3 conversion increased with increasing temperature and decreasing initial NH_3 concentration. Significant levels of NO_X emissions were observed during NH_3 oxidation, which increased with increasing temperature. From the experimental results, it is speculated that the stainless-steel in the thermocouple bundle may have catalysed NH_3 dissociation and thus changed the reaction chemistry during NH_3 oxidation.

Keywords

Ammonia, NH_3 Dissociation, NH_3 Oxidation, Flow Reactor, Nitrogen Oxides (NO_X), Thermal Effects

1. Introduction

Recent years have seen a growing interest in ammonia (NH_3) as a potential renewable and carbon-free fuel when it is produced from renewable hydrogen [1]. Unlike conventional fossil fuels, the combustion of NH_3 does not emit carbon oxides (CO, CO_2), sulphur oxides (SO_X), or particulate matter (PM) emissions. Figure 1 indicates the volumetric and gravimetric energy densities of various fuels. Ammonia is typically stored and transported as a liquid at −33˚C and 1.1 ~ 1.5 bar [2] [3] under which conditions the respective gravimetric and volumetric energy densities are 22.5 MJ/kg and 15.6 MJ/L [4] [5]. The energy densities of NH_3 are thus comparable to several other commonly used fuels, with a volumetric energy density higher than its renewable alternative, H_2, which contends with high storage and transport costs. Several challenges face the use of NH_3 as a fuel in typical combustion systems, including high ignition energy and autoignition temperature, high lower flammability limit, slow flame propagation speed, and potential nitrogen oxides (NO_X) formation [3] [6] [7] [8] [9]. This can result in low flame stability and reduced combustion intensity which yields decreased operability and efficiency. Additionally, the potential formation and ultimate emission of NO_X associated with burning NH_3 is a major environmental concern

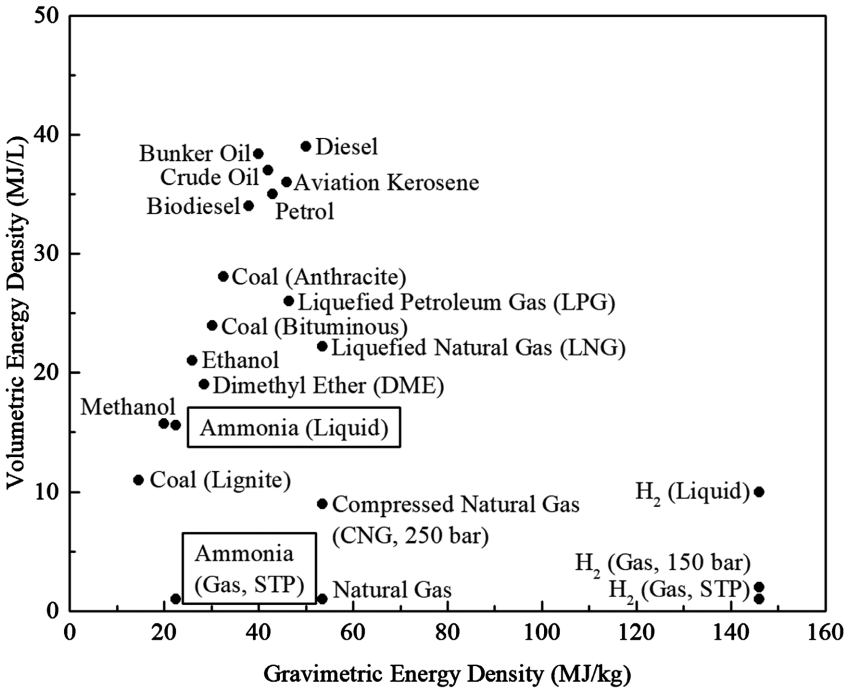

Figure 1. Comparison of volumetric and gravimetric energy densities of various fuels.

which needs to be carefully studied and, if required, countermeasures developed as it can act as a greenhouse gas, causes acid rain and urban haze, and is toxic to life [4]. Like many other commercially used fuels, NH_3 combustion involves several safety hazards including toxicity in its release or in the release of NO_X upon combustion, as well as generic flammability and explosion risks.

The Centre for Energy at The University of Western Australia has launched a significant scientific research programme to investigate combustion performance and NO_X formation during NH_3 dissociation and oxidation in several different types of reactors (flow reactor, fixed-bed reactor, and fluidised-bed reactor) in an aim to realise improved combustion efficiencies [10] [11]. The present contribution reports a preliminary experimental investigation into the thermal effects during NH_3 dissociation and oxidation in a flow reactor. Based on the reactor temperature profiles and effluent gas composition data for varying inlet NH_3 and O_2 concentrations in argon (Ar) and furnace set temperatures, some interesting phenomenological observations can be made, thereby assisting in the interpretation and understanding of heat release intensities of the prevailing reactions.

2. Experimental

Figure 2 shows a schematic diagram of the experimental system. Gases were dosed to the system using mass flow controllers before being combined in a mixer containing small quartz granules and fed into the reactor from the top. The quartz tube reactor (25.4 mm OD and 3 mm wall thickness) was held in a split-tube furnace (model TCH-T1200-II) which provided heating to the reactor across two 200 mm zones. A bundle of 8 thermocouples attached to a central DIA = 2 mm stainless-steel rod was positioned along the central axis of the reactor to provide a temperature profile that was originally considered as a means of identifying the thermal effects associated with NH_3 dissociation and oxidation. The reactor exit stream gas lines were heated to and maintained at ~150˚C using an electric heating tape to prevent condensation of water vapour. H_2, O_2, N_2, and NH_3 were measured using a modified gas chromatograph (Agilent 78980A) while NO was measured using a chemiluminescent analyser (Thermo Scientific 42i-HL). The NO analyser requires the removal of H_2O and NH_3 from the gas sample before entering the analyser and this was achieved via the three-stage process: knock-out container, water bubbler, and Perma Pure dryer (model PD-50T-12MSS).

This experimental campaign was designed to observe the impact of initial NH_3 concentration and furnace temperature on the thermal effects during NH_3 dissociation and oxidation. The flow rate and equivalence ratios were fixed at 1500 mL/min and $\phi = 1$, respectively. Initial NH_3 concentrations of 5%, 10%, and 15% were tested. Before introducing reactants into the feed, the system was purged with 1500 mL/min Ar and, when the temperature profile stabilised, the data acquisition system was initiated and MFCs set to the desired experimental conditions. A steady-state was deemed to be achieved when the temperature profile

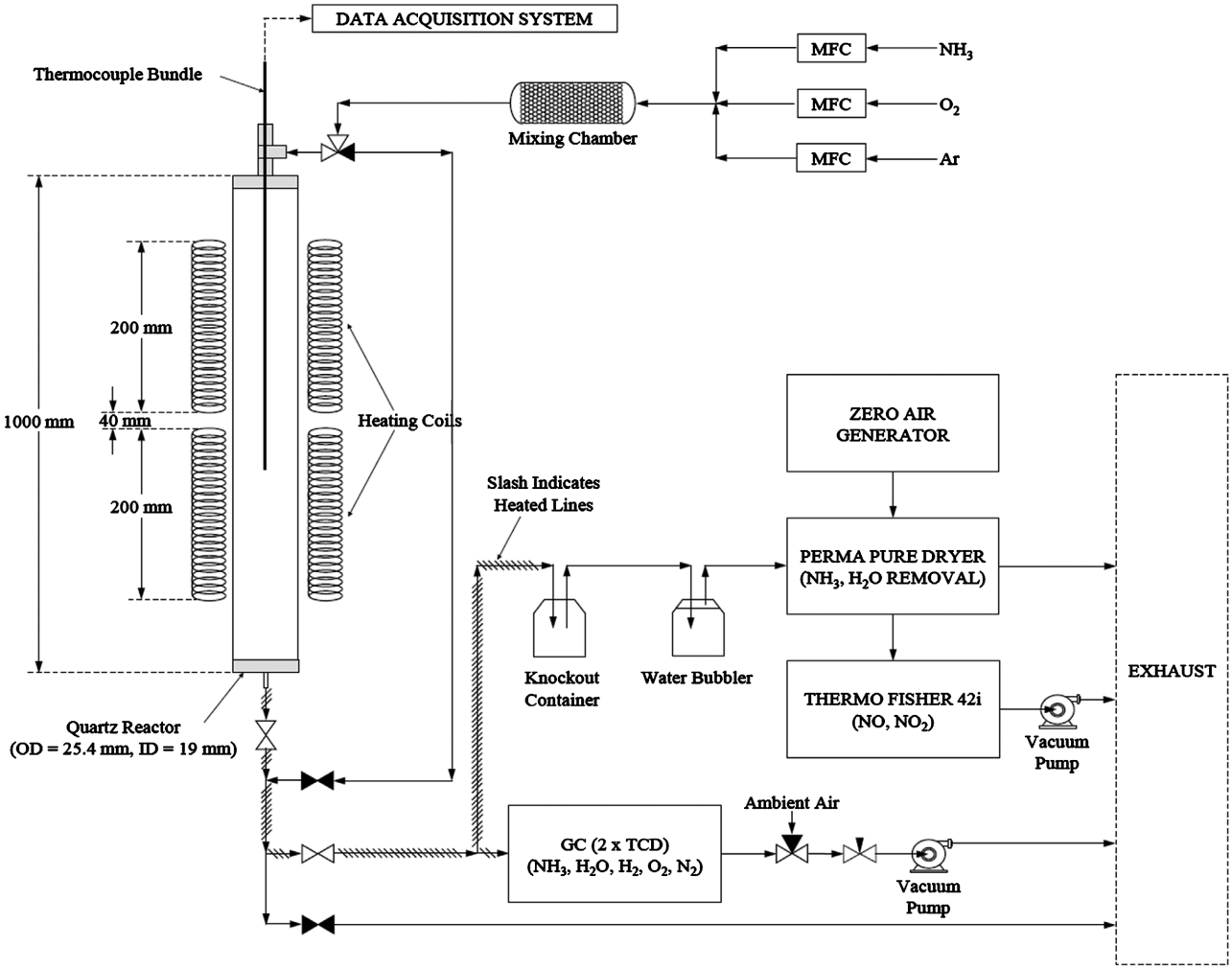

Figure 2. A schematic diagram of the experimental system.

was once again found to stabilise, following which the gas concentration data was collected. Species concentration measurement was taken 3 times to ensure accuracy and reproducibility of data.

3. Results and Discussion

Ammonia dissociation and oxidation are considered separately to understand the role of dissociation in the more complex oxidation reaction. The use of the thermocouple bundle was intended to provide a qualitative indication of the location and extent of the reactions which, coupled with the NH_3, O_2, N_2, and NO outlet data, provides the tools for an insightful appreciation of reaction characteristics.

Since the temperature profile along the reactor length is a key indicator of reaction behaviour, reference temperature profiles were collected for an inert environment with Ar passing through the reactor at a flow rate of 1500 mL/min at the different furnace set temperatures. These temperature profiles, as depicted in Figure 3, provide the baselines for the interpretation of temperature changes in the reactor during NH_3 dissociation and oxidation.

3.1. NH_3 Dissociation

The reactor temperature and exit stream species concentration profiles during NH_3 dissociation at different initial NH_3 concentrations and furnace set temperatures are presented in Figure 4 and Figure 5, respectively. Plots of NH_3

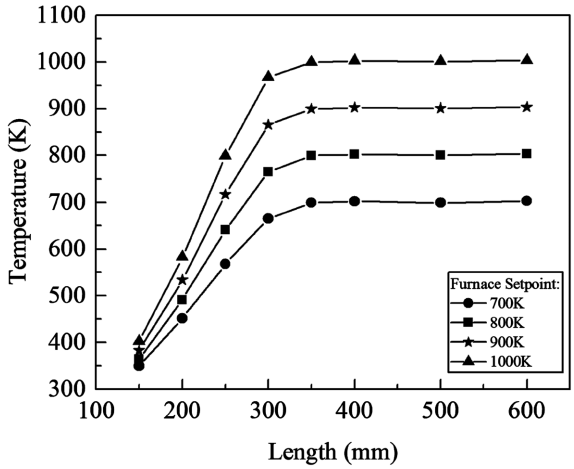

Figure 3. Reactor reference temperature profiles at different furnace temperatures (Ar flow of 1500 mL/min).

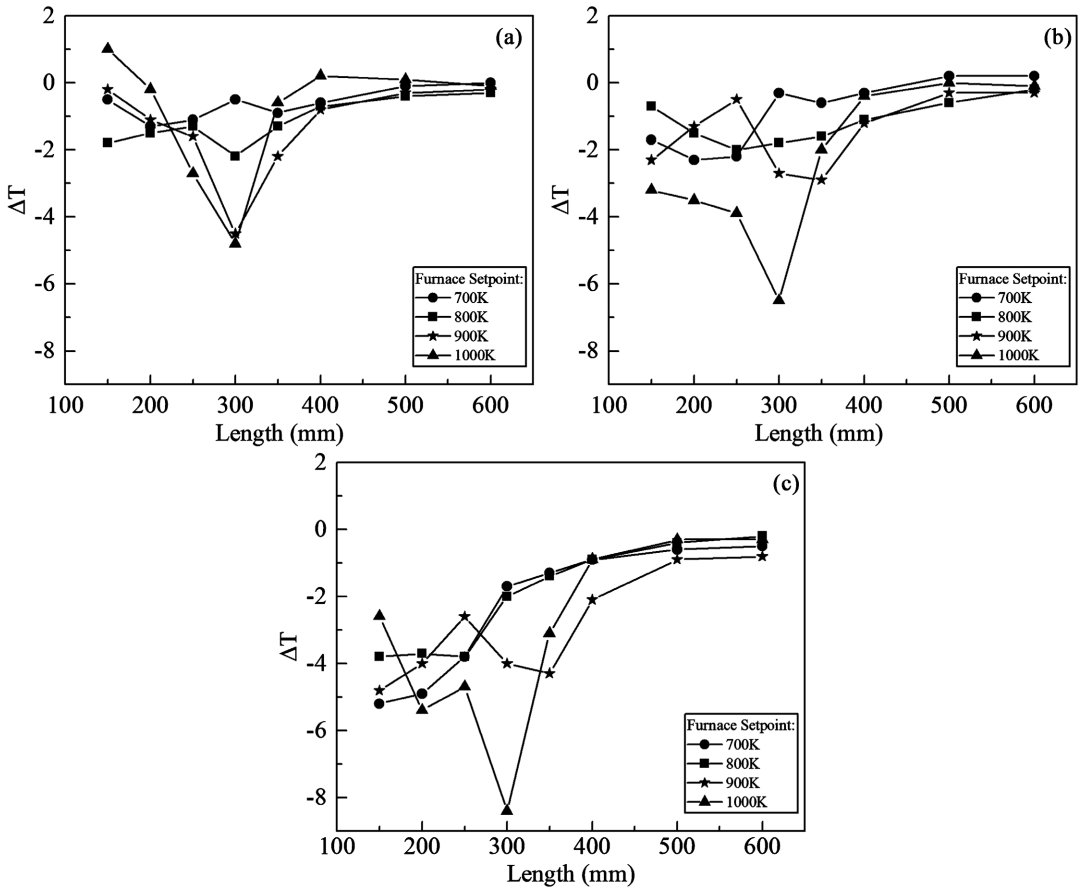

Figure 4. Reactor temperature profiles during NH_3 dissociation at different furnace temperatures for initial NH_3 concentrations of (a) 5%, (b) 10%, and (c) 15%.

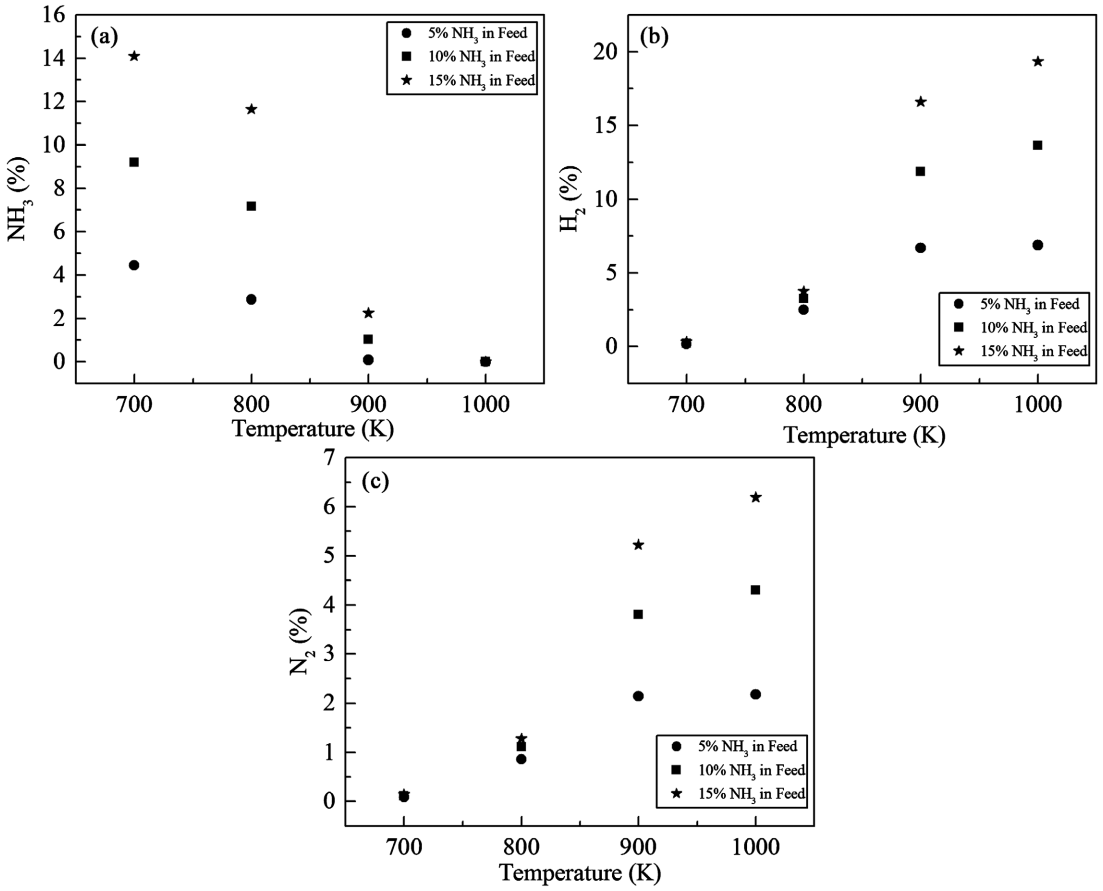

Figure 5. Reactor exit stream species concentration versus furnace temperature during NH_3 dissociation for (a) NH_3, (b) H_2, and (c) N_2.

conversion, N_2 yield, and H_2 yield, calculated as a result of the species concentration data, are offered in Figure 6.

It is evident that the endothermic NH_3 dissociation reaction took place under all experimental conditions, with the conversion/yield plots following generic 'S' curves, where majority of the reaction occurred at 800 K - 900 K before completion at 1000 K. As expected, the NH_3 conversion and N_2 and H_2 yield increased with increasing furnace temperature for all initial conditions. The preliminary NH_3 dissociation experiments in a flow reactor without the presence of the thermocouple bundle indicated that, for a 5% NH_3 in Ar feed, the dissociation reaction would proceed to ~1%, ~1.4%, and ~2.8% completion for furnace temperatures of 1150 K, 1250 K, and 1400 K, respectively [10]. Other studies showed reaction onset temperatures of 1100 K - 1200 K with full NH_3 conversion at 1700 K [12] [13]. Clearly, there is a large disparity between the dataset from the present work and those documented in the literature [10] [12] [13], indicating that the stainless-steel thermocouple bundle catalysed NH_3 dissociation.

The greatest change in thermocouple temperatures (ΔT = reference temperature − reaction temperature) was observed at 200 mm - 400 mm for all initial NH_3 concentrations and furnace temperatures and so it is deduced that a substantial part

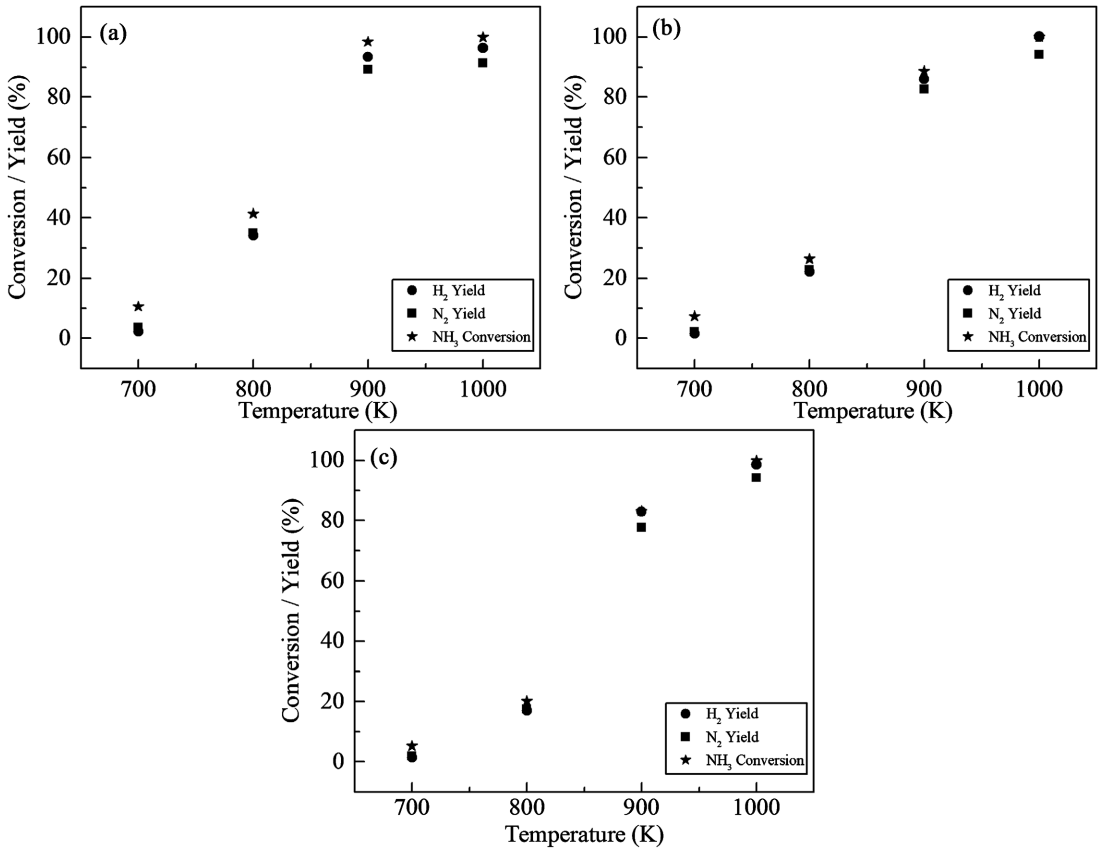

Figure 6. Conversion/yield during NH_3 dissociation at different furnace temperatures for initial NH_3 concentrations of (a) 5%, (b) 10%, and (c) 15%.

of the dissociation reaction occurred in this region. The majority of the reaction was detected around 300 mm (start of the furnace heated zone), indicating that while the thermocouples located upstream of 300 mm were operating at temperatures noticeably below the furnace setpoint, small amounts of NH_3 conversion was still occurring in this location, while positions further downstream of 300 mm experienced endothermic heat of the residual reaction.

At higher initial NH_3 concentrations, an overall reduction in the thermocouple temperatures was observed, suggesting that as the reaction was operating at lower temperatures, decreased NH_3 conversion is expected. This is supported by the experimental observation herein and elsewhere [12] of lower initial NH_3 concentrations achieving increased NH_3 conversion at equivalent furnace temperatures when compared to higher initial NH_3 concentrations.

Figure 7 illustrates the elemental nitrogen balance during NH_3 dissociation at different furnace set temperatures and Figure 8 shows the corresponding H_2:N_2 ratios. The nitrogen balance is defined as:

$$\text{Nitrogen Balance \%} = \frac{\text{Moles of NH}_3\text{in Product} + 2\times\text{Moles of N}_2\text{ in Product}}{\text{Moles of NH}_3\text{ in Feed}}\times 100 \quad (1)$$

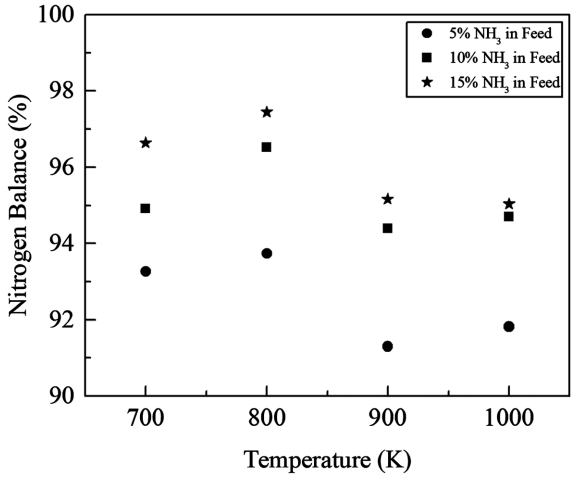

Figure 7. Elemental nitrogen balance during NH_3 dissociation at different furnace set temperatures.

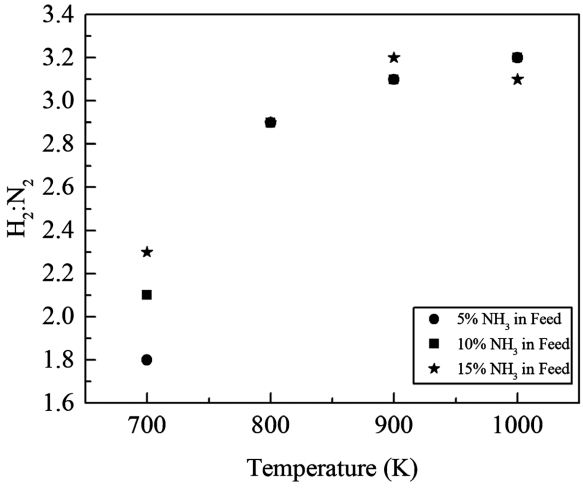

Figure 8. H_2:N_2 ratio in the reactor exit stream as measured at different furnace set temperatures.

The nitrogen balance improves with increasing NH_3 in the feed which is primarily attributed to larger GC peak area, leading to more accurate NH_3 and N_2 measurement. The H_2:N_2 ratio is poor at 700 K due to little NH_3 conversion and thus a greater uncertainty due to nearly undetectable H_2 and N_2 peak areas, resulting in enormous measurement error. Reasonable NH_3 conversion occurred between 800 K and 1000 K which is reflected by $2.9 < H_2{:}N_2 < 3.2$. Given the indicative purpose of the findings presented in this paper and the uncertainties associated with the experimental setup (particularly small peak area GC measurement), the species concentration data can be accepted with a reasonable degree of confidence.

3.2. NH_3 Oxidation

The reactor temperature and exit stream species concentration profiles during NH_3 oxidation at different initial NH_3 concentrations and furnace set temperatures are presented in **Figure 9** and **Figure 10**, respectively. Plots of NH_3

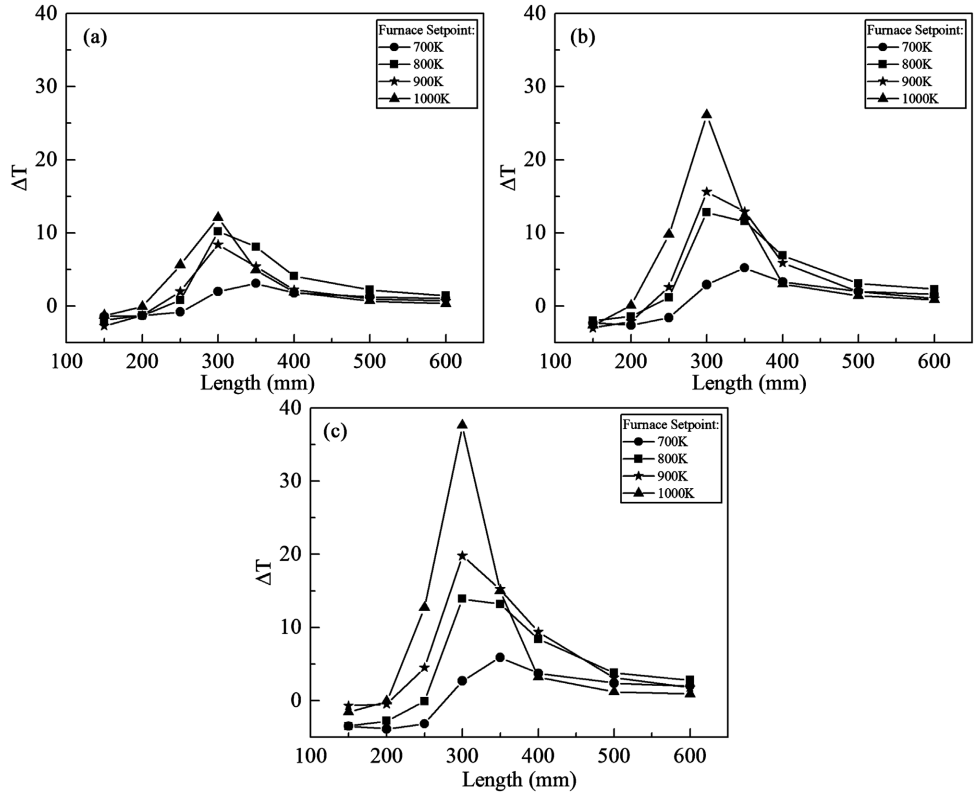

Figure 9. Reactor temperature profiles during NH_3 oxidation at different furnace temperatures for initial NH_3 concentrations of (a) 5%, (b) 10%, and (c) 15%.

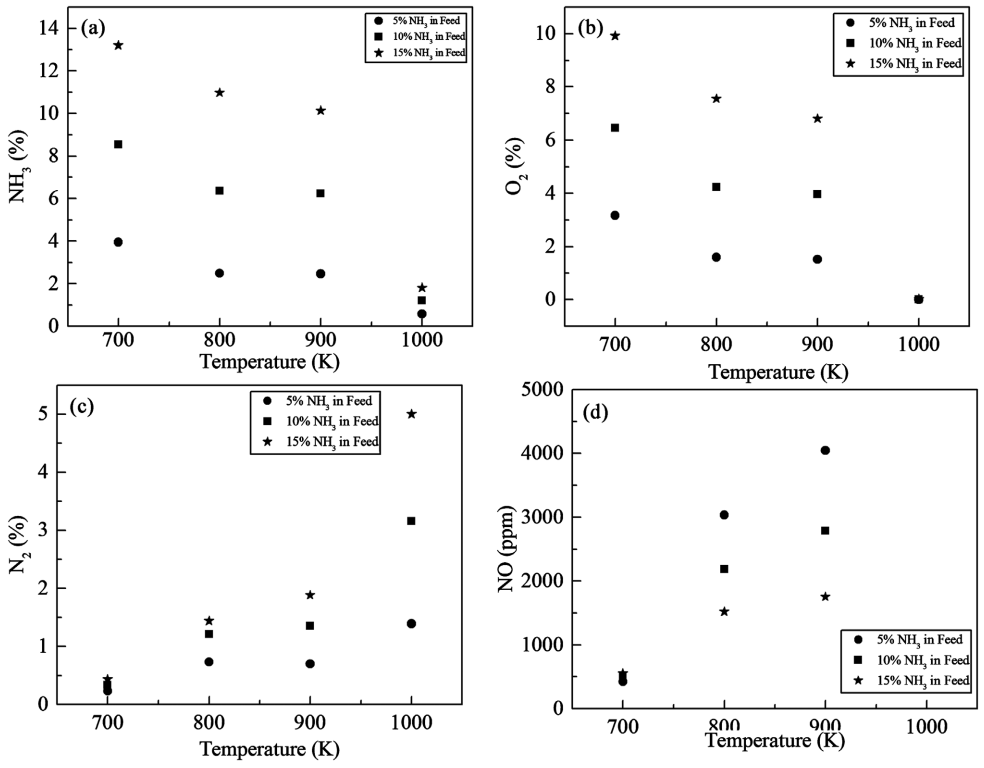

Figure 10. Reactor exit stream species concentration versus furnace temperature during NH_3 oxidation for (a) NH_3, (b) O_2, (c) N_2, and (d) NO.

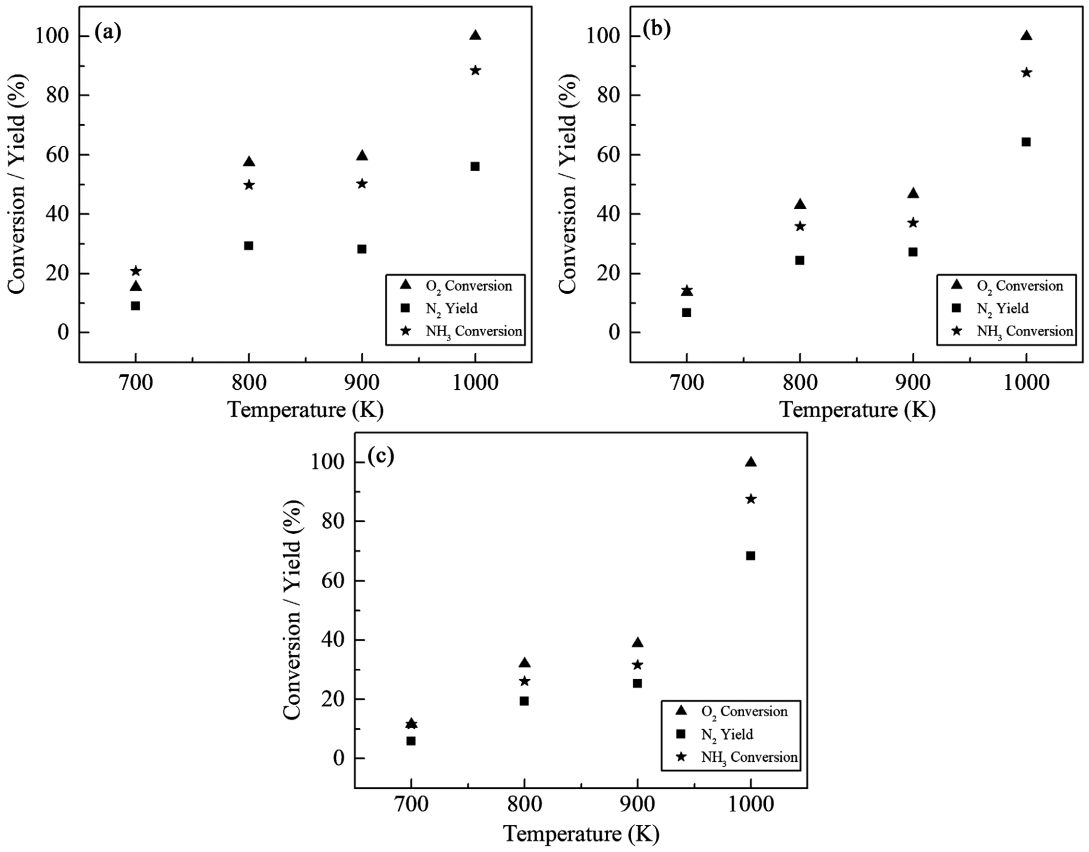

Figure 11. Conversion/yield during NH_3 oxidation at different furnace temperatures for initial NH_3 concentrations of (a) 5%, (b) 10%, and (c) 15%.

conversion, O_2 conversion, and N_2 yield, calculated as a result of the species concentration data, are offered in Figure 11.

The consumption of NH_3 and O_2, production of N_2, and overall increase in temperature along the reactor, suggest that the exothermic NH_3 oxidation reaction occurred under all conditions tested, with significant reactant conversion between 900 K and 1000 K. According to the temperature profiles, it appears that the dissociation reaction took place early in the reactor (indicated by decreases in temperatures at 150 mm, 200 mm, and 250 mm under some conditions), while the exothermic oxidation reaction (indicated by increases in temperatures) proceeds further downstream with the greatest change in temperature being shown at 300 mm (start of the furnace heated zone). Like the dissociation reaction, lower initial NH_3 concentrations resulted in greater reactant conversion at equivalent furnace temperatures compared to higher initial NH_3 concentrations, thus highlighting the significance of NH_3 dissociation in the oxidative environment.

For the various NH_3 feed concentrations tested (except 5% NH_3 at 700 K), O_2 conversion was the highest, followed closely by NH_3 conversion and subsequently N_2 yield. As reactant conversion and product yield increase, however, the gap widens between the NH_3 or O_2 conversion and the N_2 yield. This coincides with the formation of N_2O (observed on the GC) and high quantities of NO being read by the NO_X analyser, which is particularly evident at 1000 K, for

example, where NO readings were out of the NO_X analyser instrument range (>10,000 ppm) and a prominent new peak was observed on the GC, suggesting that there was a high quantity of NO_X present in the product. This notion is supported in the nitrogen balance (calculated according to Equation (1)) which becomes worse with increasing temperature (and thus NH_3 conversion), as indicated in **Figure 12**.

As the furnace set temperature and thus reactant conversion and product yield increased, the NO level in the exit stream (depicted in **Figure 10(d)**) also increased, which is expected as increasing temperature enhances the rate of oxidation of NH_3 which, in the absence of N_2 in the feed stream, is the only source of NO. Additionally, the NO in the flue increased with decreasing initial NH_3 concentration. This is very interesting and may be attributed to NO reduction by NH_3 at higher initial NH_3 concentrations via selective catalytic reduction (SCR) [14] [15] [16] where the stainless-steel thermocouple bundle may serve as a catalyst, or by selective non-catalytic reduction mechanisms [17] [18] [19].

One piece of our previous work on NH_3 oxidation in a flow reactor indicated vastly different results to those observed herein, reporting an onset reaction temperature of ~1300 K, and reaction completion at ~1400 K for 5.3% NH_3 (at ϕ = 1.0) in the feed [11]. This data indicated negligible NO_X formation until 1300 K, above which NO was found to range from 350 - 600 ppm. Other papers have indicated the onset temperatures of reaction between 1000 K and 1200 K, and significantly lower NO levels than those in the present work [13] [20] [21]. The discrepancies between the data of other papers and that presented herein can only be attributed to the presence of the stainless-steel thermocouple bundle which catalysed NH_3 dissociation and oxidation leading to lower onset reaction temperatures and greater NO formation.

3.3. Interference of the Thermocouple Bundle

A comparison of the dissociation and oxidation NH_3 conversion trends, as

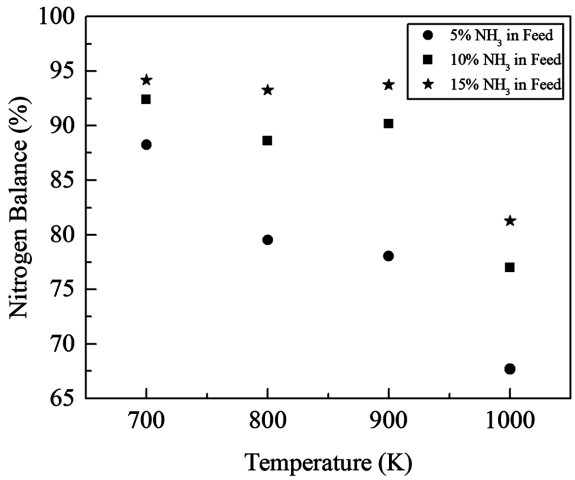

Figure 12. Elemental nitrogen balance during NH_3 oxidation at different furnace set temperatures.

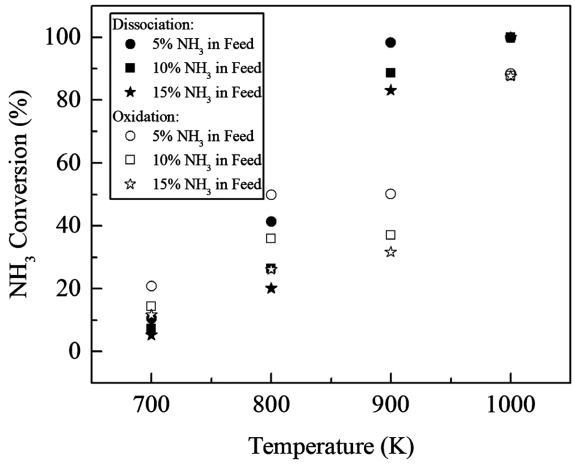

Figure 13. NH_3 conversion during dissociation and oxidation (calculated from measured NH_3 in the exit stream) at different furnace set temperatures.

depicted in **Figure 13**, produce some peculiar observations from this experimental work. At furnace temperatures of 700 K and 800 K, the NH_3 oxidation runs returned slightly higher NH_3 conversions than the dissociation runs, however, at elevated furnace temperatures, greater NH_3 conversion during dissociation than during oxidation was observed. At 900 K, for example, the NH_3 conversion in oxidation was approximately half of the NH_3 conversion in dissociation and at 1000 K, dissociation proceeded to full completion while oxidation only experienced ~88% NH_3 conversion. While the reasons underpinning these observations are only speculative, it is hypothesised that the stainless-steel sheaths of the thermocouples and the central stainless-steel rod to which the thermocouples were attached catalysed NH_3 dissociation [22] and thus changed the reaction chemistry during NH_3 oxidation. Iron is known to catalyse NH_3 synthesis at relatively low temperatures [23] [24] [25] and catalyse NH_3 dissociation at high temperatures [26] [27] [28] so it is not surprising that greater NH_3 dissociation was observed. During the NH_3 oxidation runs, partial NH_3 dissociation took place before the reacting mixture reached the heating zone of the reactor assembly, where the presence of H_2 from NH_3 dissociation is expected to have preferentially reacted with O_2, leaving less O_2 available to oxidise the remaining NH_3.

In both dissociation and oxidation experimental runs, the heat conduction and catalytic effects of the stainless-steel thermocouple bundle should not be ignored. Assuming the thermocouple bundle provides no catalytic activity, the temperature profile may not necessarily be the same should the experiments have been conducted without such *in-situ* temperature measurement as heat can be conducted along the thermocouple bundle thereby providing heating or cooling effects to the reactor gas and thus altering the reaction behaviour, as observed. Additionally, it is anticipated that the stainless-steel provided a catalytic effect on the chemical reactions as the data presented herein shows equivalently higher NH_3 conversion and elevated NO formation compared to other reports including our own previous work [10] [11] which do not utilise a thermocouple

bundle. Although it is expected to influence the reaction, the thermocouple bundle is a simple and easy *in-situ* means to observe the thermal effects during NH_3 dissociation and oxidation to provide valuable insight into the location and extent of the endothermicity or exothermicity of reactions. However, future experimental work aimed to study the reaction mechanisms of NH_3 oxidation and combustion must not use bare thermocouples in the reacting stream.

4. Conclusion

Ammonia dissociation and oxidation and associated NO emission in a flow reactor fitted with a thermocouple bundle has been experimentally observed for varying NH_3 inlet concentrations and reaction temperatures. Both NH_3 dissociation and oxidation were observed to take place between 700 K and 1000 K, with increasing furnace temperature resulting in increasing NH_3 conversion. For NH_3 dissociation, the reactant conversion and product yield vs furnace temperature plots followed generic "S" curve trends with increasing furnace temperature leading to increasing reactant conversion and product yield. This set of experiments indicated a nitrogen balance of >90% and a H_2:N_2 ratio of ~3 for all experimental runs, indicating strong validity of the experimental system and confidence in the collected data. For NH_3 oxidation, thermocouple measurements were able to provide insight into the reaction characteristics and demonstrated that NH_3 dissociation preceded its oxidation. During NH_3 oxidation, NO was observed to increase with increasing temperature, with values >10,000 ppm at 88% NH_3 conversion (1000 K). Interestingly, as temperature and thus NH_3 conversion increased, NH_3 dissociation was more prominent than its oxidation which is expected to be largely attributed to the catalytic effect of the stainless-steel thermocouple bundle which has also been observed to increase NH_3 conversion and NO emission for all experiments conducted herein. This work thus offers an important scientific contribution in determining the characteristics of NH_3 dissociation and oxidation in a flow reactor containing a stainless-steel thermocouple bundle and provides a warning for future researchers to be aware of the high temperature catalytic influence that stainless-steel is expected to have in NH_3 studies.

Acknowledgements

This work receives financial support from the Australian Research Council under the Discovery Projects Scheme (DP210103766 and DP220100116) and the Future Energy Export CRC (FEnEX CRC Project # 21.RP2.0059). S.R. Holden receives a Research Training Program Stipend Scholarship, and an Ad Hoc Postgraduate Top up Scholarship from the UWA Centre for Energy.

Conflicts of Interest

The authors declare no conflicts of interest regarding the publication of this paper.

References

[1] Riahi, K. and Roehrl, R.A. (2000) Energy Technology Strategies for Carbon Dioxide Mitigation and Sustainable Development. *Environmental Economics and Policy Studies*, **3**, 89-123. https://doi.org/10.1007/BF03354032

[2] Hignett, T.P. (1985) Transportation and Storage of Ammonia. In: Hignett, T.P., Eds., *Fertilizer Manual*, Springer, Dordrecht, 73-82. https://doi.org/10.1007/978-94-017-1538-6_7

[3] Ullman, F. (2000) Ullmann's Encyclopedia of Industrial Chemistry. Wiley-VCH, Weinheim.

[4] Valera-Medina, A., Xiao, H., Owen-Jones, M., David, W.I.F. and Bowen, P.J. (2018) Ammonia for Power. *Progress in Energy and Combustion Science*, **69**, 63-102. https://doi.org/10.1016/j.pecs.2018.07.001

[5] Zamfirescu, C. and Dincer, I. (2009) Ammonia as a Green Fuel and Hydrogen Source for Vehicular Applications. *Fuel Processing Technology*, **90**, 729-737. https://doi.org/10.1016/j.fuproc.2009.02.004

[6] Appl, M. (1999) Ammonia: Principles and Industrial Practice. Wiley-VCH, Weinheim. https://doi.org/10.1002/9783527613885

[7] Flank, W.H., Abraham, M.A. and Matthews, M.A. (2009) Innovations in Industrial and Engineering Chemistry: A Century of Achievements and Prospects for the New Millennium. American Chemical Society, Washington DC. https://doi.org/10.1021/bk-2009-1000

[8] Modak, J.M. (2011) Haber Process for Ammonia Synthesis. *Resonance*, **16**, 1159-1167. https://doi.org/10.1007/s12045-011-0130-0

[9] Smith, C., Hill, A.K. and Torrente-Murciano, L. (2020) Current and Future Role of Haber–Bosch Ammonia in a Carbon-Free Energy Landscape. *Energy & Environmental Science*, **13**, 331-344. https://doi.org/10.1039/C9EE02873K

[10] Zhang, R., Wang, J., Zhang, Y., Cheng, F., Liu, Y., Gao, J., Holden, S.R. and Zhang, D. (2022) An Experimental Study of Ammonia Dissociation in a Fixed-Bed Reactor Packed with Quartz Particles. *Clearwater Clean Energy Conference*, Clearwater, 1-4 August 2022, 1-8.

[11] Huo, Y., Zhang, R., Zhu, S., Gao, J., Holden, S.R., Zhu, M., Zhang, Z. and Zhang, D. (2022) A Preliminary Experimental Investigation into Ammonia Oxidation in a Fixed-Bed. *International Journal of Energy for a Clean Environment*, **23**, 23-37. https://doi.org/10.1615/InterJEnerCleanEnv.2022039811

[12] Benés, M., Pozo, G., Abián, M., Millera, Á., Bilbao, R. and Alzueta, M.U. (2021) Experimental Study of the Pyrolysis of NH_3 under Flow Reactor Conditions. *Energy & fuels*, **35**, 7193-7200. https://doi.org/10.1021/acs.energyfuels.0c03387

[13] Manna, M.V., Sabia, P., Ragucci, R. and de Joannon, M. (2020) Oxidation and Pyrolysis of Ammonia Mixtures in Model Reactors. *Fuel*, **264**, Article ID: 116768. https://doi.org/10.1016/j.fuel.2019.116768

[14] Gómez-García, M.A., Pitchon, V. and Kiennemann, A. (2005) Pollution by Nitrogen Oxides: An Approach to NO_X Abatement by Using Sorbing Catalytic Materials. *Environment International*, **31**, 445-467. https://doi.org/10.1016/j.envint.2004.09.006

[15] Husnain, N., Wang, E., Li, K., Anwar, M.T., Mehmood, A., Gul, M., Li, D. and Mao, J. (2019) Iron Oxide-Based Catalysts for Low-Temperature Selective Catalytic Reduction of NO_X with NH_3. *Reviews in Chemical Engineering*, **35**, 239-264. https://doi.org/10.1515/revce-2017-0064

[16] Li, Z., Chen, G., Shao, Z., Zhang, H. and Guo, X. (2022) The Effect of Iron Content on the Ammonia Selective Catalytic Reduction Reaction (NH_3-SCR) Catalytic Performance of FeO_x/SAPO-34. *International Journal of Environmental Research and Public Health*, **19**, Article 14749. https://doi.org/10.3390/ijerph192214749

[17] Javed, M.T., Ahmed, Z., Ibrahim, M.A. and Irfan, N. (2008) A Comparative Kinetic Study of SNCR Process Using Ammonia. *Brazilian Journal of Chemical Engineering*, **25**, 109-117. https://doi.org/10.1590/S0104-66322008000100012

[18] Locci, C., Vervisch, L., Farcy, B., Domingo, P. and Perret, N. (2018) Selective Non-Catalytic Reduction (SNCR) of Nitrogen Oxide Emissions: A Perspective from Numerical Modeling. *Flow, Turbulence and Combustion*, **100**, 301-340. https://doi.org/10.1007/s10494-017-9842-x

[19] Sorrels, J.L., Randall, D.D., Fry, C.R. and Schaffner, K.S. (2019) Selective Noncatalytic Reduction. U.S. Environmental Protection Agency.

[20] Nakamura, H., Hasegawa, S. and Tezuka, T. (2017) Kinetic Modeling of Ammonia/Air Weak Flames in a Micro Flow Reactor with a Controlled Temperature Profile. *Combustion and Flame*, **185**, 16-27. https://doi.org/10.1016/j.combustflame.2017.06.021

[21] Stagni, A., Cavallotti, C., Arunthanayothin, S., Song, Y., Herbinet, O., Battin-Leclerc, F. and Faravelli, T. (2020) An Experimental, Theoretical and Kinetic-Modeling Study of the Gas-Phase Oxidation of Ammonia. *Reaction Chemistry & Engineering*, **5**, 696-711. https://doi.org/10.1039/C9RE00429G

[22] Feng, P., Lee, M., Wang, D. and Suzuki, Y. (2023) Ammonia Thermal Decomposition on Quartz and Stainless Steel Walls. *International Journal of Hydrogen Energy*. https://doi.org/10.1016/j.ijhydene.2023.04.106

[23] Jennings, J.R. (1991) Catalytic Ammonia Synthesis, Fundamentals and Practice. Plenum Press, New York. https://doi.org/10.1007/978-1-4757-9592-9

[24] Liu, H. (2013) Ammonia Synthesis Catalysts: Innovation and Practice. World Scientific Publishing Co. Pte. Ltd and Chemical Industry Press, Singapore and Beijing.

[25] Liu, H. (2014) Ammonia Synthesis Catalyst 100 Years: Practice, Enlightenment and Challenge. *Chinese Journal of Catalysis*, **35**, 1619-1640. https://doi.org/10.1016/S1872-2067(14)60118-2

[26] Arabczyk, W. and Zamłynny, J. (1999) Study of the Ammonia Decomposition over Iron Catalysts. *Catalysis Letters*, **60**, 167-171. https://doi.org/10.1023/A:1019007024041

[27] Pelka, R., Moszyńska, I. and Arabczyk, W. (2009) Catalytic Ammonia Decomposition Over Fe/Fe_4N. *Catalysis Letters*, **128**, 72-76. https://doi.org/10.1007/s10562-008-9758-0

[28] Lucentini, I., Garcia, X., Vendrell, X. and Llorca, J. (2021) Review of the Decomposition of Ammonia to Generate Hydrogen. *Industrial & Engineering Chemistry Research*, **60**, 18560-18611. https://doi.org/10.1021/acs.iecr.1c00843